ATLAS Paper Draft

ANA-HDBS-2019-08
Version 1.0
Target journal: JHEP

Comments are due by: 31 March 2023

Supporting internal notes

4ℓ+MET internal note: https://cds.cern.ch/record/2788797

Search for heavy resonances in final states with 4ℓ and missing transverse energy or jets in pp collisions at $\sqrt{s} = 13$ TeV with the ATLAS detector

A search for a new heavy boson produced via gluon-fusion in the four-lepton channel with missing transverse energy or jets is performed. The search uses proton-proton collision data equivalent to an integrated luminosity of 139 fb^{-1} at a centre-of-mass energy of 13 TeV collected by the ATLAS detector between 2015 and 2018 at the Large Hadron Collider. The heavy boson, R (A), decays to an S (Z) boson, and another lighter Higgs-like boson, H, decays to two Z bosons. The S boson is assumed to decay to dark matter, and the associated Z boson decays either to two leptons or inclusively. The mass spectrum studied is 390–1300 (320–1300) GeV for the R (A) boson and 220–1000 GeV for the H boson. The S boson mass is fixed at 160 GeV to reduce the number of free parameters. No significant deviation from the Standard Model backgrounds is observed. The results are interpreted as upper limits at a 95% confidence level on the $\sigma(gg \to R) \times \mathrm{B}(R \to SH) \times \mathrm{B}(H \to ZZ) \times \mathrm{B}(ZZ \to 4\ell)$ and $\sigma(gg \to A) \times \mathrm{B}(A \to ZH) \times \mathrm{B}(H \to ZZ) \times \mathrm{B}(ZZZ \to 4\ell)$. The observed (expected) upper limits are in the range of 0.027–0.532 (0.030–0.322) fb for the $R \to SH \to 4\ell + E_{\mathrm{T}}^{\mathrm{miss}}$ model, and 0.023–0.378 (0.028–0.289) for $A \to ZH \to 4\ell + X$ model.

Document created on 24th April 2023 using ATLAS LaTeX Version 07-03-00.

Analysis Team

[*email:* atlas-ana-hdbs-2019-08-editors@cern.ch]

Abdualazem Fadol, Yaquan Fang, Theodota Lagouri, Bruce Mellado, Onesimo Mtintsilana, Xifeng Ruan, Xin Shi, Humphry Tlou

Editorial Board

Journal: JHEP

ATLAS Paper

ANA-HDBS-2019-08

24th April 2023

Draft version 1.0

Search for heavy resonances in final states with 4ℓ and missing transverse energy or jets in pp collisions at $\sqrt{s} = 13$ TeV with the ATLAS detector

The ATLAS Collaboration

A search for a new heavy boson produced via gluon-fusion in the four-lepton channel with missing transverse energy or jets is performed. The search uses proton-proton collision data equivalent to an integrated luminosity of 139 fb^{-1} at a centre-of-mass energy of 13 TeV collected by the ATLAS detector between 2015 and 2018 at the Large Hadron Collider. The heavy boson, R (A), decays to an S (Z) boson, and another lighter Higgs-like boson, H, decays to two Z bosons. The S boson is assumed to decay to dark matter, and the associated Z boson decays either to two leptons or inclusively. The mass spectrum studied is 390–1300 (320–1300) GeV for the R (A) boson and 220–1000 GeV for the H boson. The S boson mass is fixed at 160 GeV to reduce the number of free parameters. No significant deviation from the Standard Model backgrounds is observed. The results are interpreted as upper limits at a 95% confidence level on the $\sigma(gg \to R) \times \mathrm{B}(R \to SH) \times \mathrm{B}(H \to ZZ) \times \mathrm{B}(ZZ \to 4\ell)$ and $\sigma(gg \to A) \times \mathrm{B}(A \to ZH) \times \mathrm{B}(H \to ZZ) \times \mathrm{B}(ZZZ \to 4\ell)$. The observed (expected) upper limits are in the range of 0.027–0.532 (0.030–0.322) fb for the $R \to SH \to 4\ell + E_{\mathrm{T}}^{\mathrm{miss}}$ model, and 0.023–0.378 (0.028–0.289) for $A \to ZH \to 4\ell + X$ model.

Contents

1 Introduction

In 2012, the ATLAS and CMS experiments independently discovered a new particle [1, 2]. The new particle's properties are consistent with the Higgs boson proposed by the Standard Model (SM) [3–6]. Nonetheless, there are yet questions that the SM still needs to answer. For instance, the dark matter, neutrino masses and mixing, the hierarchy problem, and the strong CP problem are so far open queries [7–9]. Whether the found particle is a particle in its own right or simply a part of the Higgs sector suggested by the two-Higgs-doublet (2HDM) is until now debated [10, 11]. The 2HDM predicts the existence of five Higgs bosons: a CP-even particle like the SM Higgs boson (h), a heavier Higgs boson (H), a CP-odd particle (A), and a charged Higgs scalar ($H^{\pm}$). Another extension to the SM is a model where a real scalar boson (S) is introduced to the 2HDM (2HDM+S) [12, 13]. The S boson is assumed to be a dark matter portal and a possible source of missing transverse energy.

In this paper, our aim is to search for heavy resonances decaying to 4ℓ and missing transverse energy or jets. The search focuses on the high-mass region of the heavy bosons where the four-lepton invariant mass is above 200 GeV. Only the gluon-gluon fusion production mode is considered in this analysis. This study uses proton-proton collision data at a centre-of-mass energy of 13 TeV and integrated luminosity of 139 fb^{-1} collected by the ATLAS detector in 2015–2018 period at the Large Hadron Collider (LHC). Two different scenarios are considered for the signal model. First, the 2HDM+S model only includes a heavy resonance H and Higgs-like scalar boson S. The model is extended to cover more general situations for various missing energy magnitudes by adding one heavy scalar R, where R decays to H and S bosons with $m_R > m_H + m_S$. The H is assumed to decay to four leptons (4ℓ where ℓ could be an electron or a muon), and the S decays to SM neutrinos. The masses of the R and H bosons are varied to control the missing transverse energy, and the S mass is fixed to 160 GeV. The assumption of the S mass is motivated by the

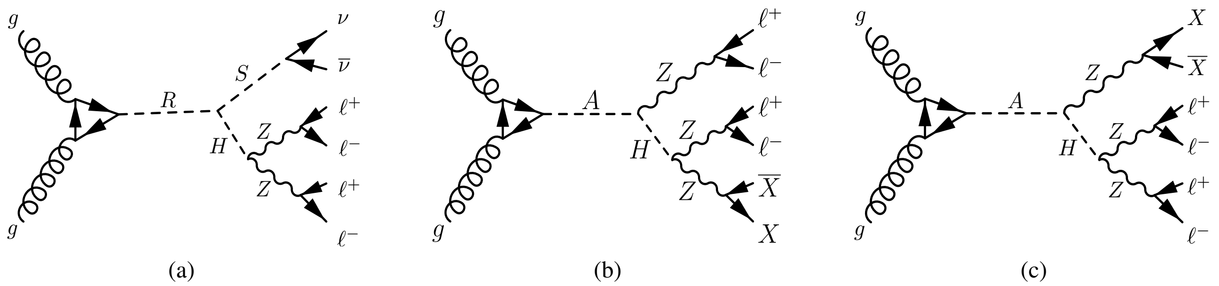

Figure 1: Feynman diagrams represent the production of heavy bosons via gluon-fusion at leading-order for (a) $R \to SH \to 4\ell + E_{\mathrm{T}}^{\mathrm{miss}}$ and (b)(c) $A \to ZH \to 4\ell + X$ ($X \equiv \nu/q/\ell^{-}$) signal models.

phenomenology study presented in Ref. [14]. However, we studied the effect of this choice and found that the S mass only affects the missing transverse energy kinematic if its mass is above 200 GeV. Therefore, fixing the S mass reduces the free parameters on the fit and simplifies the analysis. The phenomenology of the new $R \to SH$ topology can easily embed into the 2HDM+S model using a similar approach as in Ref. [12]. Second, a 2HDM-based baryogenesis scenario is considered, which generates matter and antimatter asymmetry. This model is motivated by the equal amount of matter and antimatter supposedly generated in the early universe [15]. Searches for baryogenesis were conducted at the LHC with several channels, such as $H \to hh$ [16, 17], $H \to WW/ZZ$ [18–23] and $A \to Zh$ [24, 25]. In addition, searches in the $A- > ZH- > 2\ell 2b/2\ell 2\tau$ [26–29] channels were also carried out in the LHC. In the latter case, for a strong first-order phase transition to occur in the early universe, the $m_A > m_H$ is preferred. Therefore, the $A \to ZH \to 4\ell + X$ model is added to this study to explore regions with jet activities. In this signal, A is a CP-odd scalar which decays to a CP-even scalar H and Z boson. Two decay methods are assumed for associated Z and H bosons: $Z \to X$ and $H \to ZZ \to 4\ell$, and $Z \to 2\ell$ and $H \to ZZ \to 2\ell + X$, where X could be missing transverse energy or jets.

This paper is organised as follows. The ATLAS experiment is shortly described in Section 2. Section 3 describes the data and Monte Carlo samples, followed by the object reconstruction in Section 4. Section 5 describes the analysis strategy and the signal and background modelling are discussed in Section 6. The experimental and theoretical systematic uncertainties are demonstrated in Section 7. The results are discussed in Section 8, and a conclusion is given in Section 9.

2 ATLAS detector

The ATLAS detector is a multipurpose particle physics detector at the LHC with cylindrical geometry[1] and forward-backwards symmetry [30]. It contains an inner tracker detector (ID) covered by a superconducting solenoid feeding a 2 T magnetic field, electromagnetic (EM) and hadronic calorimeters, and a muon spectrometer with superconducting magnets. The ID has a silicon pixel, a silicon microstrip tracker, a transition radiation tracker, and an insertable B-layer [31] covering the region $|\eta| < 2.5$. The calorimeter

[1] ATLAS uses a right-handed coordinate system with its origin at the nominal interaction point (IP) in the centre of the detector and the z-axis along the beam pipe. The x-axis points from the IP to the centre of the LHC ring, and the y-axis points upwards. Cylindrical coordinates (r, ϕ) are used in the transverse plane, ϕ being the azimuthal angle around the z-axis. The rapidity is defined as $y = (1/2)\ln[(E + p_z)/(E - p_z)]$, where E is the energy and p_z is the longitudinal component of the momentum along the beam pipe. The pseudorapidity is defined in terms of the polar angle θ as $\eta = -\ln\tan(\theta/2)$. Angular distance is measured in units of $\Delta R \equiv \sqrt{(\Delta\eta)^2 + (\Delta\phi)^2}$.

design includes lead/liquid-argon, steel/scintillator-tile, copper/liquid-argon, or tungsten/liquid-argon as the absorber fabric. It provides a pseudorapidity coverage of $|\eta| < 4.9$. The muon spectrometer (MS) incorporates superconducting toroidal air-core magnets around the calorimeters, which supply muon identification and momentum measurement for $|\eta| < 2.7$. A trigger system is employed at two stages to select events with an average rate of about 1 kHz for offline analysis [32].

3 Data and simulated event samples

The data used in this analysis consists of proton-proton collisions at a centre-of-mass energy of 13 GeV recorded by the ATLAS detector at the LHC from 2015 to 2018. Events are required to satisfy the data quality requirements to ensure the quality of the collected data [33–35]. After applying the event cleaning criteria, the total integrated luminosity of the entire data reached 139 fb^{-1}.

Background and signal events were simulated using Monte Carlo (MC) generators according to ATLAS detector configurations. These events were used for signal optimisation, background parametrisation, and estimation of systematic uncertainties. The $q\bar{q} \to ZZ$ background was generated using Sherpa v2.2.2 [36] with NNPDF 30 NNLO PDF set [37]. The generation was achieved with next-to-leading order (NLO) in the matrix element calculation for 0- and 1-jet final states and leading order (LO) for 2- and 3-jet final states. The accuracy was calculated with the Comix [38] and OpenLoops [39–41]. The Sherpa parton shower [42] for the merging was performed by MePs@NLO prescription [43]. Electroweak (EW) correction at NLO as a function of the ZZ invariant mass was applied [44, 45]. Similarly, the $gg \to ZZ$ process was simulated by Sherpa v2.2.2 and OpenLoops generators. Matrix elements for 0- and 1-jet at LO were calculated and merged with the Sherpa parton shower. The PDF set NNPDF 30 NNLO was used in the generation. The VVV background events, including processes such as ZZZ, ZZW, and $WWWZ$ with at least four prompt charged leptons, were simulated using Sherpa v2.2.2 with NNPDF 30 NNLO PDF set. The $q\bar{q} \to ZZ$ (EW) events, consisting of leptons and two jets, were simulated using Sherpa v2.2.2 with NNPDF 30 NNLO PDF set. Events containing four prompt charged leptons coming from $t\bar{t}V$ backgrounds ($V = Z$ or $W^{\pm}$) were modelled by MadGraph5_aMC@NLO [46] interfaced with Pythia8 [47] for the hadronisation. The $t\bar{t}$ events were generated using Powheg-Box v2 [48] with NNPDF 30 NNLO PDF set. Pythia8 was used as an interface for the showering and hadronisation with the A14 NNPDF23LO tune, and EvtGen was used to simulate B-hadron decays. Powheg-Box v2 and Pythia8 were used for the generation and hadronisation of the WZ process, respectively. The Z+jets events were modelled using Sherpa v2.2.0 generator. Matrix elements for 0- and 2-jet at NLO and 3- and 4-jet at LO were calculated with Comix and OpenLoops. For the merging, the Sherpa parton shower MePs@NLO prescription was used.

The $R \to SH \to 4\ell + E_{\mathrm{T}}^{\mathrm{miss}}$ signal was simulated using Pythia8 with A14 tune and NNPDF 23 LO PDF set. MadGraph5_aMC@NLO was used to simulate $A \to Z(\to X)H(\to 4\ell)$ and $A \to Z(\to 2\ell)H(\to 2\ell + X)$ signals with A14 tune and NNPDF 23 LO PDF set. The R mass considered is in the range of 390–1300 GeV, with the S mass fixed to 160 GeV, and the A mass is 320–1300 GeV. The H mass for both signal models is in the range of 220–1000 GeV.

4 Object reconstruction

The event selection relies on the reconstruction and identification of electrons, muons, and jets. The reconstruction and identification follow the analysis reported in Ref. [49] and are briefly summarized in the following. Electrons are reconstructed from the energy deposited in the EM calorimeter associated with the tracks found in the ID [50–52]. Muons are reconstructed from the combination of tracks found in the ID with tracks or segments of tracks found in the MS [53]. Electrons (muons) are required to have $p_{\mathrm{T}} > 4.5$ GeV ($p_{\mathrm{T}} > 5$ GeV) and $|\eta| < 2.47$ ($|\eta| < 2.7$). Jets are reconstructed from topological clusters using the anti-k_t algorithm with a radius parameter $R = 0.4$ [54]. The particle-flow algorithm [55] is used as input to the FastJet package [56]. Selected jets are required to have at least one vertex with two associated tracks with $p_{\mathrm{T}} > 500$ MeV, and the primary vertex is chosen to be the vertex reconstructed with the largest $\sum p_{\mathrm{T}}^2$. In addition, jet events must be in the central region ($|\eta| < 2.5$) with $p_{\mathrm{T}} > 20$ GeV. The effect of close-by bunch crossing (pile-up) during the p–p collision is decreased by requiring jets with $|\eta| < 2.5$ and $20 < p_{\mathrm{T}} < 60$ GeV to pass a jet-vertex-tagger multivariate discriminant requirement [57, 58]. A geometrical overlap removal between a reconstructed electron, muon, and jet is applied. A jet is removed if an electron or a muon is reconstructed within a cone size (ΔR) of 0.2 and 0.1, respectively.

5 Event categorisation

Events are classified into three distinct channels based on the flavours of the selected leptons. These channels are 4μ, $4e$ and $2\mu 2e$ and are assigned on the basis of which triggers are activated in the event. They are selected with single-lepton, dilepton and trilepton triggers, with dilepton and trilepton triggers, including electron(s)-muon(s) triggers. Single-electron triggers apply “medium” or “tight” likelihood identification, whereas multi-electron triggers apply “loose” or “medium” identification.

6 Signal and background modelling

Monte Carlo simulation (MC) is used to parametrise the constructed four leptons invariant mass ($m_{4\ell}$) distribution for the SM backgrounds. Meanwhile, the signal shape is taken directly from the MC, as demonstrated below.

6.1 Signal model

The signal line shapes are taken directly from the MC simulation. However, since a few mass points are generated for $R \to SH \to 4\ell + E_{\mathrm{T}}^{\mathrm{miss}}$ and $A \to ZH \to 4\ell + X$ signals, interpolation is needed to cover the entire ($m_{R/A}$, m_H) phase space. A linear interpolation method is described in Ref. [59] is used to get signal shapes between the generated masses in the ($m_{R/A}$, m_H) plane. Because the signal depends on the A and H masses, interpolating the signal must be done in two steps. The first step is to fix the H mass and interpolate the energy gap or the A mass. The interpolated signals along the A mass are input for a second interpolation step where the A mass is fixed, and 10 GeV varies the H mass. The same interpolating procedures are used for the $R \to SH \to 4\ell + E_{\mathrm{T}}^{\mathrm{miss}}$ signal to get the mass points between the generated samples.

6.2 Background model

The $m_{4\ell}$ shape of the backgrounds is obtained from MC simulation and parametrised using an empirical function. Four background templates are used as $q\bar{q} \to ZZ$, $gg \to ZZ$, VVV and others. The VVV has a different shape from the rest of the backgrounds, so it is kept on a different template. Backgrounds such as $q\bar{q} \to ZZ$ (EW), $t\bar{t}V$, $t\bar{t}$, Z+jets and WZ are combined in a template called others. Each of the background templates is fitted with an analytical function for $m_{4\ell}$ between 200–1200 GeV, as follows:

$$f(m_{4\ell}) = H(m_0 - m_{4\ell}) f_1(m_{4\ell})\, C_1 + H(m_{4\ell} - m_0) f_2(m_{4\ell})\, C_2, \tag{1}$$

where:

$$f_1(m_{4\ell}) = \frac{a_1 \cdot m_{4\ell} + a_2 \cdot m_{4\ell}^2}{1 + \exp\left(\frac{m_{4\ell} - a_1}{a_3}\right)} \tag{2}$$

$$f_2(m_{4\ell}) = \left(1 - \frac{m_{4\ell}}{n_C}\right)^{b_1} \cdot \left(\frac{m_{4\ell}}{n_C}\right)^{\left(b_2 + b_3 \cdot \ln\left(\frac{m_{4\ell}}{n_C}\right)\right)} \tag{3}$$

$$C_1 = \frac{1}{f_1(m_0)}, \qquad C_2 = \frac{1}{f_2(m_0)}$$

f_1 models the ZZ threshold around $2 \cdot m_Z$, and f_2 describes the high mass tail. The transition between f_1 and f_2 functions is performed by the Heaviside step function $H(x)$ around m_0, where m_0 is fixed to 260, 240, 250 and 230 for the $q\bar{q} \to ZZ$, $gg \to ZZ$, VVV, and others backgrounds, respectively. The transition point is determined by optimising the function's smoothness. A constant $n_C = 13$ TeV scales the $m_{4\ell}$ in the high mass region. C_1 and C_2 ensure the continuity of the function around the m_0 corresponding to f_1 and f_2.

7 Systematic uncertainties

8 Results

8.1 Statistical procedures

The invariant mass of the four leptons ($m_{4\ell}$) is utilised as a discriminant to examine the null and alternative hypotheses using the profile likelihood ratio technique [60]. The null hypothesis results in smoothed backgrounds that fall from the low mass range to the higher mass range of the m_{4l} distribution. In contrast, the alternative hypothesis constructs a signal structure around the H mass. The signal and background contributions in the $m_{4\ell}$ distribution are extracted via binned maximum-likelihood fits by the signal-plus background hypotheses to extract any indications for new physics. The profile likelihood function is defined by the probability of observing n events times the product sum of the weighted signal and background events, as shown below:

$$\mathcal{L}(m_{4\ell}^n | \sigma^{gg\to A/R}, \vec{\theta}) = \prod_{r=\mathrm{SR}}^{n_r} \prod_{b=\mathrm{bin}}^{n_b} \mathrm{Poisson}\left(n_{r,b} \mid S_{r,b} + \sum_{Bkg} Bkg_{r,b}(\vec{\theta})\right) \times \prod_i G_i(0|\vec{\theta}, 1), \tag{4}$$

where $\sigma^{gg\rightarrow A/R}$ represents the production cross-section of the A/R boson, and S and Bkg are the expected signal and background yields in each bin of the $m_{4\ell}$ distribution. The expected signal yields S is calculated by:

$$S = \sigma^{gg\rightarrow A/R} \times \mathrm{B}(A/R \rightarrow ZH/SH) \times \mathrm{B}(H \rightarrow ZZ) \times \mathrm{B}(ZZZ/ZZ \rightarrow 4\ell) \times (\mathrm{Accep} \times \mathrm{Effi}) \times \int L\,\mathrm{d}t, \quad (5)$$

where Accep $\times$ Effi is the acceptance times efficiency and $\int L\,\mathrm{d}t = 139\ \mathrm{fb}^{-1}$ is the integrated luminosity of the data. A collection of nuisance parameters is introduced to describe how systematic uncertainties influence the predicted number of signal and background events and the shape of the PDFs. These parameters are constrained to their nominal values within the calculated uncertainties using Gaussian constraints by $G(\vec{\theta})$. The dependency on the analysis category for each event is implied in the product by the index r. The $q\bar{q} \rightarrow ZZ$ and $gg \rightarrow ZZ$ backgrounds normalisation are set free and controlled by the μ^{ZZ} parameter per signal region. The benefit of releasing the ZZ background normalisation is to reduce the background dependency on the theory and other systematic uncertainties.

9 Conclusion

A search for new heavy resonances in the 4ℓ (ℓ could be an electron or a muon) channel with missing transverse energy or jets is performed. The search uses proton-proton collision data at a centre-of-mass energy of 13 TeV collected with the ATLAS detector from 2015 to 2018 at the Large Hadron Collider, corresponding to a total integrated luminosity of 139 fb^{-1}. The mass range for the hypothetical resonance spans between 390 (320) GeV and 2160 (2090) GeV for the R (A) boson. And the heavy boson H mass considered is between 220 GeV to 1000 GeV. Upper limits on the $\sigma \times \mathrm{BR}(R(A) \rightarrow SH(ZH)) \times \mathrm{BR}(H \rightarrow ZZ) \times \mathrm{B}(ZZ(ZZZ) \rightarrow 4\ell)$ at 95% confidence level are set. The expected (observed) upper limits of the $R \rightarrow SH \rightarrow 4\ell + E_{\mathrm{T}}^{\mathrm{miss}}$ model are in the range of 0.030–0.05 (xx–xx) fb for $(m_R,\ m_H)$ = (390, 220) GeV to $(m_R,\ m_H)$ = (1300, 1000) GeV. For the $A \rightarrow ZH \rightarrow 4\ell + X$ model, the expected (observed) upper limits are in the range of 0.028 - 0.293 (xx–xx) fb for (m_A, m_H) = (320, 220) GeV to (m_A, m_H) = (1300, 1000) GeV. The upper limits for the $A \rightarrow ZH \rightarrow 4\ell + X$ model are translated to exclusion contours in the (m_H, m_A) plane in terms of Type I and lepton-specific two-Higgs-doublet models (Type II and flipped 2HDM will be added too).

Acknowledgements

We thank CERN for the very successful operation of the LHC, as well as the support staff from our institutions without whom ATLAS could not be operated efficiently.

We acknowledge the support of ANPCyT, Argentina; YerPhI, Armenia; ARC, Australia; BMWFW and FWF, Austria; ANAS, Azerbaijan; SSTC, Belarus; CNPq and FAPESP, Brazil; NSERC, NRC and CFI, Canada; CERN; CONICYT, Chile; CAS, MOST and NSFC, China; COLCIENCIAS, Colombia; MSMT CR, MPO CR and VSC CR, Czech Republic; DNRF and DNSRC, Denmark; IN2P3-CNRS, CEA-DRF/IRFU, France; SRNSFG, Georgia; BMBF, HGF, and MPG, Germany; GSRT, Greece; RGC, Hong Kong SAR, China; ISF and Benoziyo Center, Israel; INFN, Italy; MEXT and JSPS, Japan; CNRST, Morocco; NWO, Netherlands; RCN, Norway; MNiSW and NCN, Poland; FCT, Portugal; MNE/IFA, Romania; MES of Russia and NRC KI, Russian Federation; JINR; MESTD, Serbia; MSSR, Slovakia;

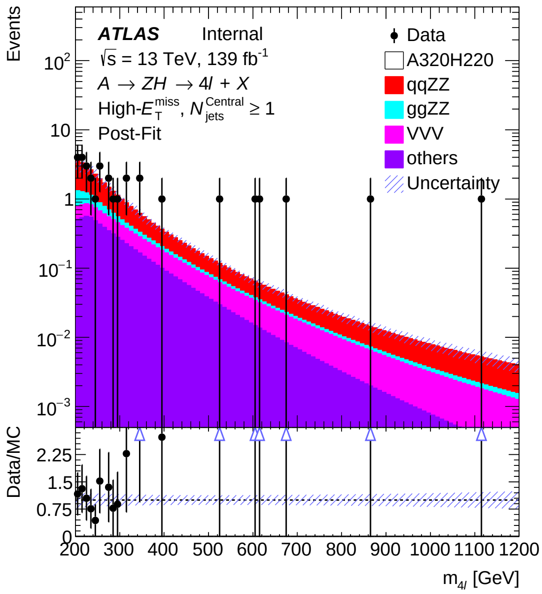

(a)

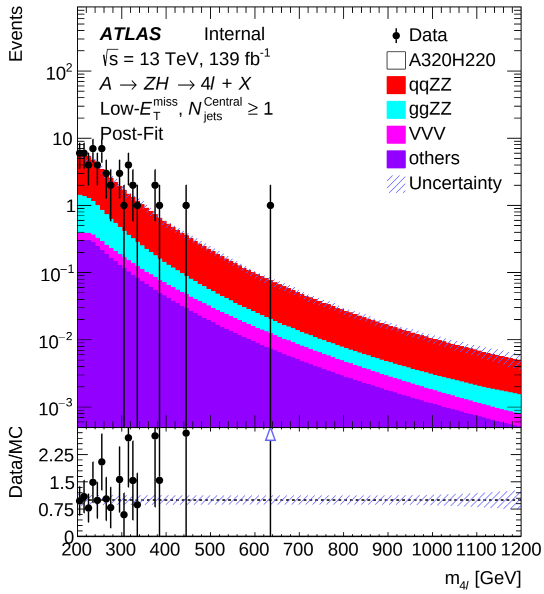

(b)

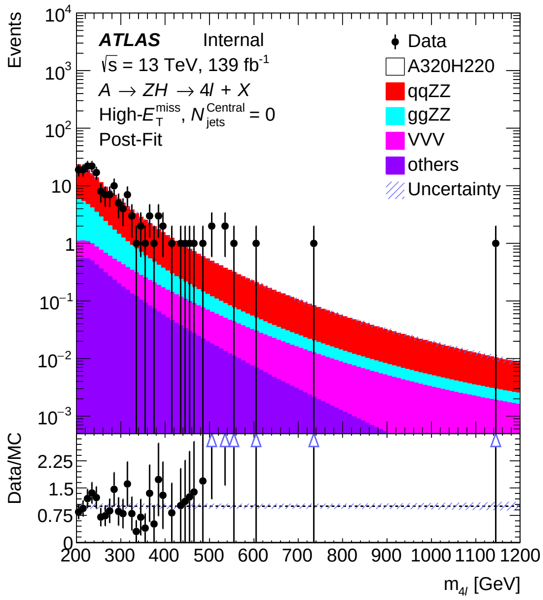

(c)

Figure 2: The $m_{4\ell}$ distributions of the $A \to ZH \to 4\ell + X$ signal with $(m_A, m_H) = (320, 220)$ GeV for different categories after signal-plus-background fit to Asimov data based on the background templates.

ARRS and MIZŠ, Slovenia; DST/NRF, South Africa; MINECO, Spain; SRC and Wallenberg Foundation, Sweden; SERI, SNSF and Cantons of Bern and Geneva, Switzerland; MOST, Taiwan; TAEK, Turkey; STFC, United Kingdom; DOE and NSF, United States of America. In addition, individual groups and members have received support from BCKDF, CANARIE, CRC and Compute Canada, Canada; COST, ERC, ERDF, Horizon 2020, and Marie Sk lodowska-Curie Actions, European Union; Investissements

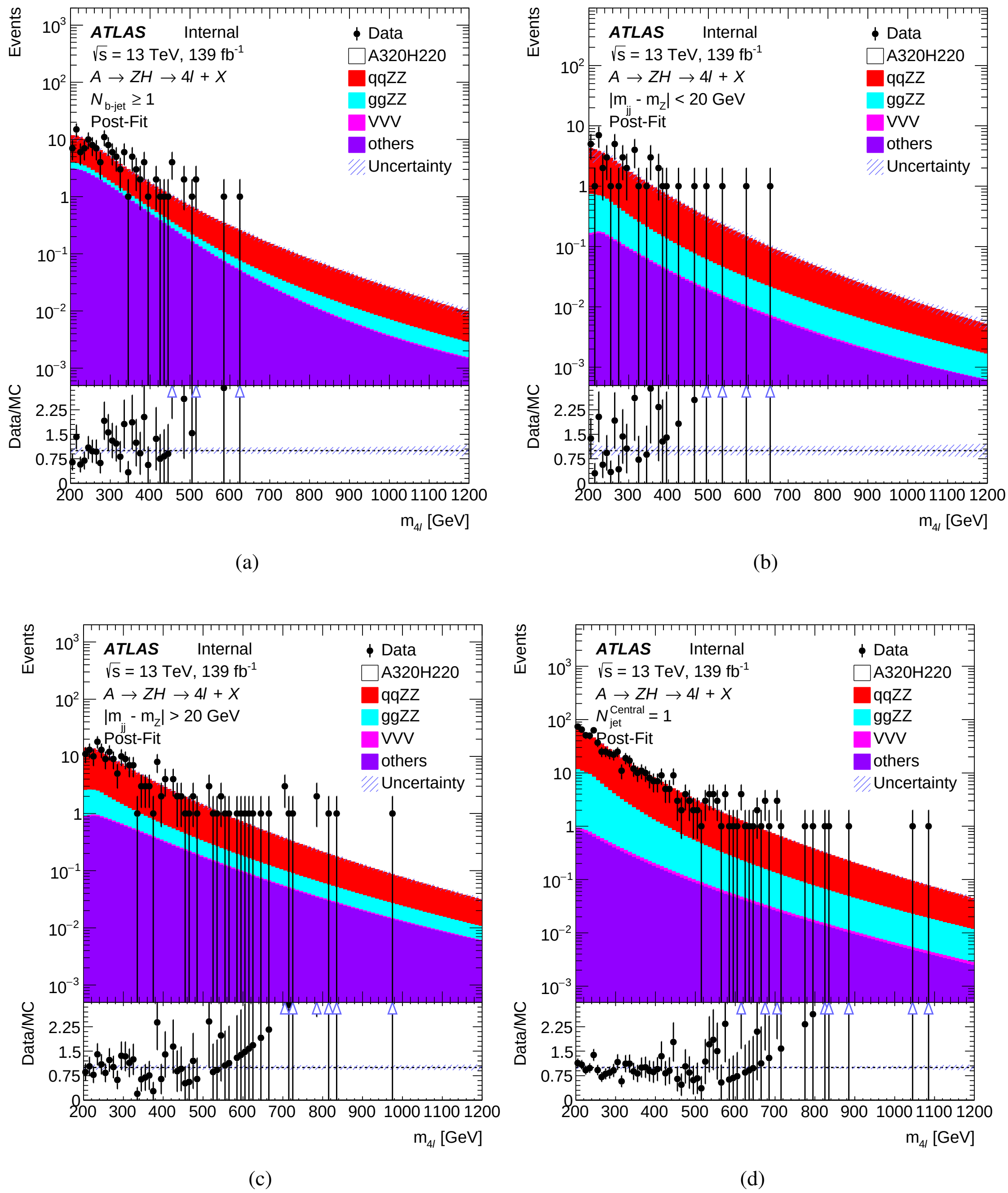

Figure 3: The $m_{4\ell}$ distributions of the $A \to ZH \to 4\ell + X$ signal with $m_A, m_H = (330, 220)$ GeV for different categories after signal-plus-background fit to Asimov data based on the background templates.

d' Avenir Labex and Idex, ANR, France; DFG and AvH Foundation, Germany; Herakleitos, Thales and Aristeia programmes co-financed by EU-ESF and the Greek NSRF, Greece; BSF-NSF and GIF, Israel; CERCA Programme Generalitat de Catalunya, Spain; The Royal Society and Leverhulme Trust, United Kingdom.

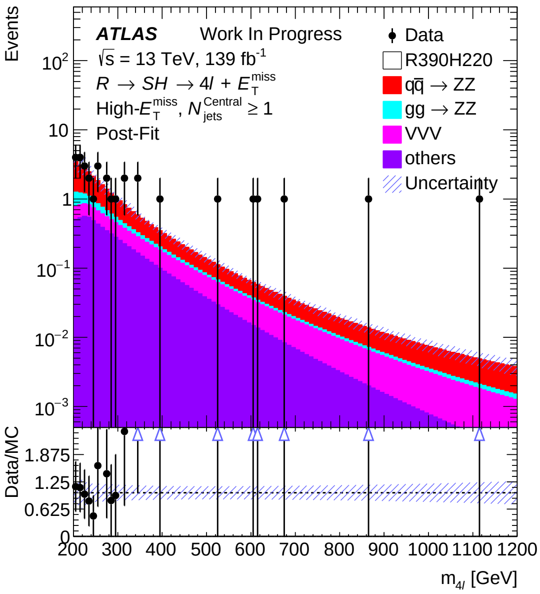

(a)

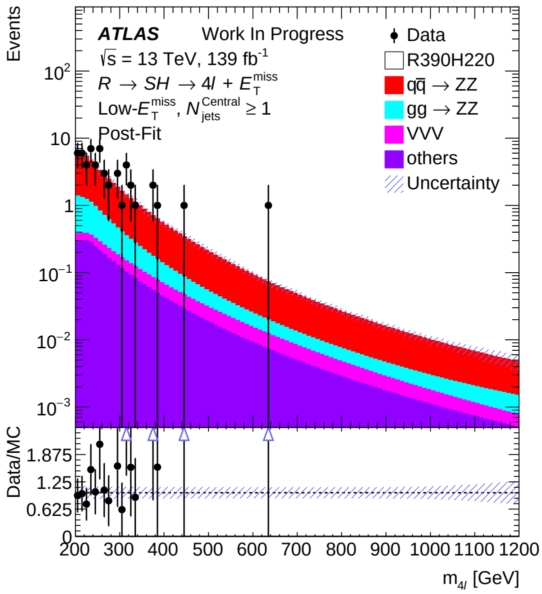

(b)

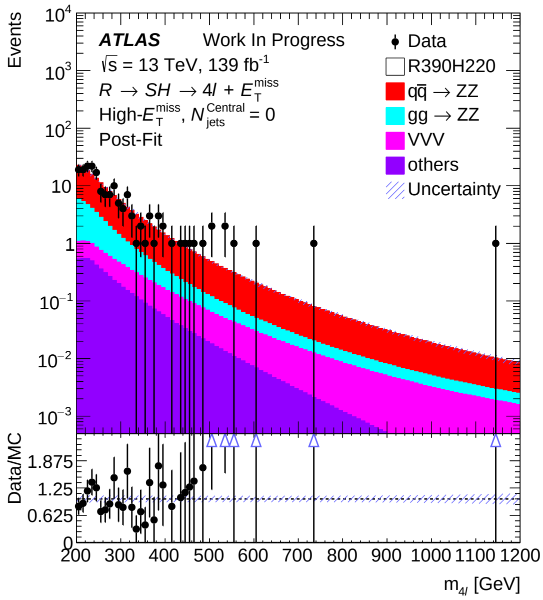

(c)

Figure 4: The $m_{4\ell}$ distributions of the $R \to SH \to 4\ell + E_{\mathrm{T}}^{\mathrm{miss}}$ signal with $m_R, m_H = (390, 220)$ GeV for different categories after signal-plus-background fit to Asimov data based on the background templates.

The crucial computing support from all WLCG partners is acknowledged gratefully, in particular from CERN, the ATLAS Tier-1 facilities at TRIUMF (Canada), NDGF (Denmark, Norway, Sweden), CC-IN2P3 (France), KIT/GridKA (Germany), INFN-CNAF (Italy), NL-T1 (Netherlands), PIC (Spain), ASGC (Taiwan), RAL (UK) and BNL (USA), the Tier-2 facilities worldwide and large non-WLCG resource providers. Major contributors of computing resources are listed in Ref. [61].

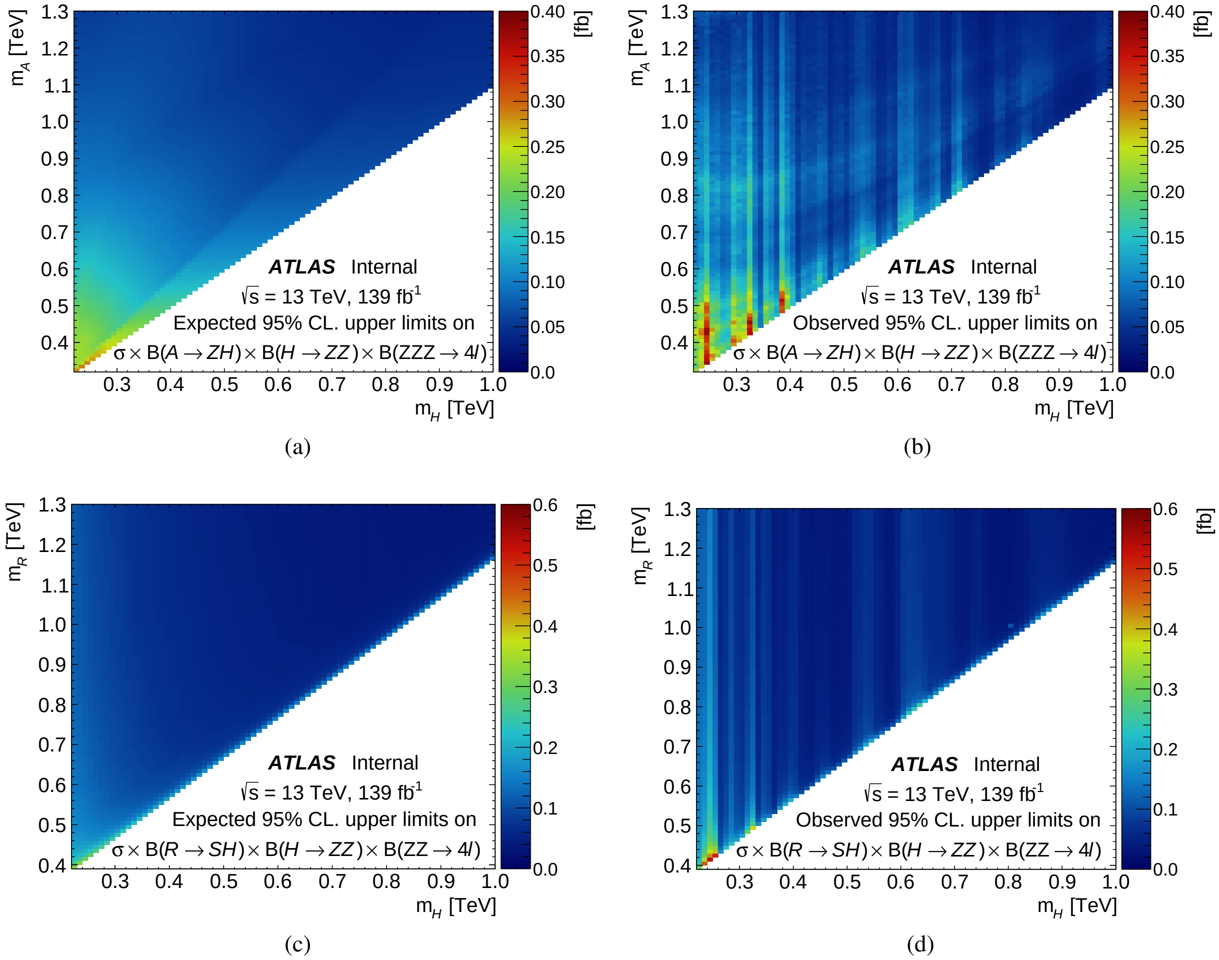

Figure 5: The expected (left) and observed (right) upper limit at 95% confidence level on (a), (b) the $\sigma \times \mathrm{BR}(A \to ZH) \times \mathrm{BR}(H \to ZZ) \times \mathrm{BR}(ZZZ \to 4\ell)$, and (c), (d) $\sigma \times \mathrm{BR}(R \to SH) \times \mathrm{BR}(H \to ZZ) \times \mathrm{BR}(ZZ \to 4\ell)$ on (m_H, m_A) (left) and $(m_H,\, m_R)$ (right) planes.

References

[1] ATLAS Collaboration, *Observation of a new particle in the search for the Standard Model Higgs boson with the ATLAS detector at the LHC*, Phys. Lett. B **716** (2012) 1, arXiv: 1207.7214 [hep-ex] (cit. on p. 2).

[2] CMS Collaboration, *Observation of a new boson at a mass of 125 GeV with the CMS experiment at the LHC*, Phys. Lett. B **716** (2012) 30, arXiv: 1207.7235 [hep-ex] (cit. on p. 2).

[3] ATLAS Collaboration, *Measurements of the Higgs boson production and decay rates and coupling strengths using pp collision data at $\sqrt{s} = 7$ and 8 TeV in the ATLAS experiment*, Eur. Phys. J. C **76** (2016) 6, arXiv: 1507.04548 [hep-ex] (cit. on p. 2).

[4] ATLAS Collaboration, *Study of the spin and parity of the Higgs boson in diboson decays with the ATLAS detector*, Eur. Phys. J. C **75** (2015) 476, arXiv: 1506.05669 [hep-ex] (cit. on p. 2), Erratum: Eur. Phys. J. C **76** (2016) 152.

[5] CMS Collaboration, *Precise determination of the mass of the Higgs boson and tests of compatibility of its couplings with the standard model predictions using proton collisions at* 7 *and* 8 *TeV*, Eur. Phys. J. C **75** (2015) 212, arXiv: 1412.8662 [hep-ex] (cit. on p. 2).

[6] CMS Collaboration, *Constraints on the spin-parity and anomalous HVV couplings of the Higgs boson in proton collisions at* 7 *and* 8 *TeV*, Phys. Rev. D **92** (2015) 012004, arXiv: 1411.3441 [hep-ex] (cit. on p. 2).

[7] H. E. Haber and G. L. Kane, *The Search for Supersymmetry: Probing Physics Beyond the Standard Model*, Phys. Rept. **117** (1985) 75 (cit. on p. 2).

[8] N. Arkani-Hamed, S. Dimopoulos and G. R. Dvali, *The Hierarchy problem and new dimensions at a millimeter*, Phys. Lett. B **429** (1998) 263, arXiv: hep-ph/9803315 (cit. on p. 2).

[9] G. F. Giudice, *Naturally Speaking: The Naturalness Criterion and Physics at the LHC*, 2008, arXiv: 0801.2562 [hep-ph] (cit. on p. 2).

[10] G. C. Branco et al., *Theory and phenomenology of two-Higgs-doublet models*, Phys. Rept. **516** (2012) 1, arXiv: 1106.0034 [hep-ph] (cit. on p. 2).

[11] T. D. Lee, *A Theory of Spontaneous T Violation*, Phys. Rev. D **8** (1973) 1226, ed. by G. Feinberg (cit. on p. 2).

[12] S. von Buddenbrock et al., *Phenomenological signatures of additional scalar bosons at the LHC*, Eur. Phys. J. C **76** (2016) 580, arXiv: 1606.01674 [hep-ph] (cit. on pp. 2, 3).

[13] M. Muhlleitner, M. O. P. Sampaio, R. Santos and J. Wittbrodt, *The N2HDM under Theoretical and Experimental Scrutiny*, JHEP **03** (2017) 094, arXiv: 1612.01309 [hep-ph] (cit. on p. 2).

[14] S. von Buddenbrock et al., *Multi-lepton signatures of additional scalar bosons beyond the Standard Model at the LHC*, J. Phys. G **45** (2018) 115003, arXiv: 1711.07874 [hep-ph] (cit. on p. 3).

[15] A. G. Cohen, D. B. Kaplan and A. E. Nelson, *Progress in electroweak baryogenesis*, Ann. Rev. Nucl. Part. Sci. **43** (1993) 27, arXiv: hep-ph/9302210 (cit. on p. 3).

[16] ATLAS Collaboration, *Combination of searches for Higgs boson pairs in pp collisions at $\sqrt{s}$ =13 TeV with the ATLAS detector*, Phys. Lett. B **800** (2020) 135103, arXiv: 1906.02025 [hep-ex] (cit. on p. 3).

[17] CMS Collaboration, *Combination of searches for Higgs boson pair production in proton-proton collisions at $\sqrt{s}$ = 13 TeV*, Phys. Rev. Lett. **122** (2019) 121803, arXiv: 1811.09689 [hep-ex] (cit. on p. 3).

[18] ATLAS Collaboration, *Searches for heavy ZZ and ZW resonances in the $\ell\ell qq$ and $\nu\nu qq$ final states in pp collisions at $\sqrt{s}$ =* 13 *TeV with the ATLAS detector*, JHEP **03** (2018) 009, arXiv: 1708.09638 [hep-ex] (cit. on p. 3).

[19] ATLAS Collaboration, *Search for WW/WZ resonance production in $\ell\nu qq$ final states in pp collisions at $\sqrt{s}$ = 13 TeV with the ATLAS detector*, JHEP **03** (2018) 042, arXiv: 1710.07235 [hep-ex] (cit. on p. 3).

[20] ATLAS Collaboration, *Search for heavy diboson resonances in semileptonic final states in pp collisions at $\sqrt{s}$ =* 13 *TeV with the ATLAS detector*, Eur. Phys. J. C **80** (2020) 1165, arXiv: 2004.14636 [hep-ex] (cit. on p. 3).

[21] ATLAS Collaboration, *Search for diboson resonances in hadronic final states in 139 fb^{-1} of pp collisions at $\sqrt{s}$ =* 13 *TeV with the ATLAS detector*, JHEP **09** (2019) 091, [Erratum: JHEP 06, 042 (2020)], arXiv: 1906.08589 [hep-ex] (cit. on p. 3).

[22] CMS Collaboration, *Search for a heavy Higgs boson decaying to a pair of W bosons in proton-proton collisions at $\sqrt{s}$ = 13 TeV*, JHEP **03** (2020) 034, arXiv: 1912.01594 [hep-ex] (cit. on p. 3).

[23] CMS Collaboration, *Search for a new scalar resonance decaying to a pair of Z bosons in proton-proton collisions at $\sqrt{s}$ = 13 TeV*, JHEP **06** (2018) 127, [Erratum: JHEP 03, 128 (2019)], arXiv: 1804.01939 [hep-ex] (cit. on p. 3).

[24] ATLAS Collaboration, *Search for heavy resonances decaying into a W or Z boson and a Higgs boson in final states with leptons and b-jets in 36 fb^{-1} of $\sqrt{s}$ = 13 TeV pp collisions with the ATLAS detector*, JHEP **03** (2018) 174, [Erratum: JHEP 11, 051 (2018)], arXiv: 1712.06518 [hep-ex] (cit. on p. 3).

[25] CMS Collaboration, *Search for a heavy pseudoscalar Higgs boson decaying into a 125 GeV Higgs boson and a Z boson in final states with two tau and two light leptons at $\sqrt{s}$ = 13 TeV*, JHEP **03** (2020) 065, arXiv: 1910.11634 [hep-ex] (cit. on p. 3).

[26] CMS Collaboration, *Search for neutral resonances decaying into a Z boson and a pair of b jets or τ leptons*, Phys. Lett. B **759** (2016) 369, arXiv: 1603.02991 [hep-ex] (cit. on p. 3).

[27] A. M. Sirunyan et al., *Search for new neutral Higgs bosons through the $H\rightarrow ZA \rightarrow \ell^+\ell^-\mathrm{b\bar{b}}$ process in pp collisions at $\sqrt{s}$ = 13 TeV*, JHEP **03** (2020) 055, arXiv: 1911.03781 [hep-ex] (cit. on p. 3).

[28] ATLAS Collaboration, *Search for a heavy Higgs boson decaying into a Z boson and another heavy Higgs boson in the $\ell\ell bb$ final state in pp collisions at $\sqrt{s}$ = 13 TeV with the ATLAS detector*, Phys. Lett. B **783** (2018) 392, arXiv: 1804.01126 [hep-ex] (cit. on p. 3).

[29] ATLAS Collaboration, *Search for a heavy Higgs boson decaying into a Z boson and another heavy Higgs boson in the $\ell\ell bb$ and $\ell\ell WW$ final states in pp collisions at $\sqrt{s}$ = 13 TeV with the ATLAS detector*, Eur. Phys. J. C **81** (2021) 396, arXiv: 2011.05639 [hep-ex] (cit. on p. 3).

[30] ATLAS Collaboration, *The ATLAS Experiment at the CERN Large Hadron Collider*, JINST **3** (2008) S08003 (cit. on p. 3).

[31] ATLAS Collaboration, *Study of the mechanical stability of the ATLAS Insertable B-Layer*, ATL-INDET-PUB-2015-001, 2015, URL: https://cds.cern.ch/record/2022587 (cit. on p. 3).

[32] ATLAS Collaboration, *Performance of the ATLAS trigger system in 2015*, Eur. Phys. J. C **77** (2017) 317, arXiv: 1611.09661 [hep-ex] (cit. on p. 4).

[33] ATLAS Collaboration, *Operation and performance of the ATLAS semiconductor tracker*, JINST **9** (2014) P08009, arXiv: 1404.7473 [hep-ex] (cit. on p. 4).

[34] ATLAS Collaboration, *Monitoring and data quality assessment of the ATLAS liquid argon calorimeter*, JINST **9** (2014) P07024, arXiv: 1405.3768 [hep-ex] (cit. on p. 4).

[35] ATLAS Collaboration, *Selection of jets produced in 13 TeV proton–proton collisions with the ATLAS detector*, ATLAS-CONF-2015-029, 2015, URL: https://cds.cern.ch/record/2037702 (cit. on p. 4).

[36] E. Bothmann et al., *Event Generation with Sherpa 2.2*, SciPost Phys. **7** (2019) 034, arXiv: 1905.09127 [hep-ph] (cit. on p. 4).

[37] R. D. Ball et al., *Parton distributions for the LHC Run II*, JHEP **04** (2015) 040, arXiv: 1410.8849 [hep-ph] (cit. on p. 4).

[38] S. Höche, F. Krauss, S. Schumann and F. Siegert, *QCD matrix elements and truncated showers*, JHEP **05** (2009) 053, arXiv: 0903.1219 [hep-ph] (cit. on p. 4).

[39] A. Denner, S. Dittmaier and L. Hofer, *Collier: a fortran-based Complex One-Loop LIbrary in Extended Regularizations*, Comput. Phys. Commun. **212** (2017) 220, arXiv: 1604.06792 [hep-ph] (cit. on p. 4).

[40] F. Buccioni et al., *OpenLoops 2*, Eur. Phys. J. C **79** (2019) 866, arXiv: 1907.13071 [hep-ph] (cit. on p. 4).

[41] F. Cascioli, P. Maierhöfer and S. Pozzorini, *Scattering Amplitudes with Open Loops*, Phys. Rev. Lett. **108** (2012) 111601, arXiv: 1111.5206 [hep-ph] (cit. on p. 4).

[42] S. Schumann and F. Krauss, *A Parton shower algorithm based on Catani-Seymour dipole factorisation*, JHEP **03** (2008) 038, arXiv: 0709.1027 [hep-ph] (cit. on p. 4).

[43] S. Höche, F. Krauss, M. Schönherr and F. Siegert, *QCD matrix elements + parton showers: The NLO case*, JHEP **04** (2013) 027, arXiv: 1207.5030 [hep-ph] (cit. on p. 4).

[44] B. Biedermann, A. Denner, S. Dittmaier, L. Hofer and B. Jäger, *Electroweak corrections to $pp \to \mu^+\mu^-e^+e^- + X$ at the LHC: a Higgs background study*, Phys. Rev. Lett. **116** (2016) 161803, arXiv: 1601.07787 [hep-ph] (cit. on p. 4).

[45] B. Biedermann, A. Denner, S. Dittmaier, L. Hofer and B. Jager, *Next-to-leading-order electroweak corrections to the production of four charged leptons at the LHC*, JHEP **01** (2017) 033, arXiv: 1611.05338 [hep-ph] (cit. on p. 4).

[46] J. Alwall, M. Herquet, F. Maltoni, O. Mattelaer and T. Stelzer, *MadGraph 5 : Going Beyond*, JHEP **06** (2011) 128, arXiv: 1106.0522 [hep-ph] (cit. on p. 4).

[47] T. Sjöstrand et al., *An Introduction to PYTHIA 8.2*, Comput. Phys. Commun. **191** (2015) 159, arXiv: 1410.3012 [hep-ph] (cit. on p. 4).

[48] S. Alioli, P. Nason, C. Oleari and E. Re, *A general framework for implementing NLO calculations in shower Monte Carlo programs: the POWHEG BOX*, JHEP **06** (2010) 043, arXiv: 1002.2581 [hep-ph] (cit. on p. 4).

[49] ATLAS Collaboration, *Search for heavy resonances decaying into a pair of Z bosons in the $\ell^+\ell^-\ell'^+\ell'^-$ and $\ell^+\ell^-\nu\bar{\nu}$ final states using 139 fb^{-1} of proton–proton collisions at $\sqrt{s} = 13$ TeV with the ATLAS detector*, Eur. Phys. J. C **81** (2021) 332, arXiv: 2009.14791 [hep-ex] (cit. on p. 5).

[50] ATLAS Collaboration, *Electron and photon performance measurements with the ATLAS detector using the 2015–2017 LHC proton-proton collision data*, JINST **14** (2019) P12006, arXiv: 1908.00005 [hep-ex] (cit. on p. 5).

[51] ATLAS Collaboration, *Electron reconstruction and identification in the ATLAS experiment using the 2015 and 2016 LHC proton-proton collision data at $\sqrt{s}$ = 13 TeV*, Eur. Phys. J. C **79** (2019) 639, arXiv: 1902.04655 [physics.ins-det] (cit. on p. 5).

[52] ATLAS Collaboration, *Improved electron reconstruction in ATLAS using the Gaussian Sum Filter-based model for bremsstrahlung*, ATLAS-CONF-2012-047, 2012, URL: https://cds.cern.ch/record/1449796 (cit. on p. 5).

[53] ATLAS Collaboration, *Muon reconstruction performance of the ATLAS detector in proton–proton collision data at $\sqrt{s}$ =13 TeV*, Eur. Phys. J. C **76** (2016) 292, arXiv: 1603.05598 [hep-ex] (cit. on p. 5).

[54] M. Cacciari, G. P. Salam and G. Soyez, *The anti-k_t jet clustering algorithm*, JHEP **04** (2008) 063, arXiv: 0802.1189 [hep-ph] (cit. on p. 5).

[55] ATLAS Collaboration, *Jet reconstruction and performance using particle flow with the ATLAS Detector*, Eur. Phys. J. C **77** (2017) 466, arXiv: 1703.10485 [hep-ex] (cit. on p. 5).

[56] M. Cacciari, G. P. Salam and G. Soyez, *FastJet User Manual*, Eur. Phys. J. C **72** (2012) 1896, arXiv: 1111.6097 [hep-ph] (cit. on p. 5).

[57] ATLAS Collaboration, *Performance of pile-up mitigation techniques for jets in pp collisions at $\sqrt{s} = 8$ TeV using the ATLAS detector*, Eur. Phys. J. C **76** (2016) 581, arXiv: 1510.03823 [hep-ex] (cit. on p. 5).

[58] ATLAS Collaboration, *Tagging and suppression of pileup jets with the ATLAS detector*, ATLAS-CONF-2014-018, 2014, URL: https://cds.cern.ch/record/1700870 (cit. on p. 5).

[59] A. L. Read, *Linear interpolation of histograms*, Nucl. Instrum. Meth. A **425** (1999) 357 (cit. on p. 5).

[60] G. Cowan, K. Cranmer, E. Gross and O. Vitells, *Asymptotic formulae for likelihood-based tests of new physics*, Eur. Phys. J. C **71** (2011) 1554, arXiv: 1007.1727 [physics.data-an] (cit. on p. 6), Erratum: Eur. Phys. J. C **73** (2013) 2501.

[61] ATLAS Collaboration, *ATLAS Computing Acknowledgements*, ATL-GEN-PUB-2016-002, URL: https://cds.cern.ch/record/2202407 (cit. on p. 10).